Wood Veneer Species Recognition Using Markovian Textural Features

Michal Haindl(✉) and Pavel Vácha

The Institute of Information Theory and Automation,
Czech Academy of Sciences, Prague, Czech Republic
{haindl,vacha}@utia.cz

Abstract. A mobile Android application that can automatically recognize wood species from a low quality mobile phone photo under varying illumination conditions is presented. The wood recognition is based on the Markovian, spectral, and illumination invariant textural features. The method performance was verified on a wood database, which contains veneers from sixty-six varied European and exotic wood species. The Markovian features improvement of the correct wood recognition rate is about 40% compared to the best alternative - the Local Binary Patterns features.

Keywords: Wood recognition · Textural features · Illumination invariants · Surface reflectance field · Bidirectional texture function

1 Introduction

Each type of wood has its own specific physical, aesthetic and economic properties; thus correct identification of wood species is required in numerous practical applications, from construction industry, manufacturing, furniture design, and restoration to pricing evaluation of wooden items. Fast, reliable, and practical recognition of wood species is therefore important, having potential impacts in a range of areas, including: the intended application, construction safety, and detecting illegal logging of endangered species. The traditional method of identifying wood species involves manual browsing through digital wooden veneer catalogues and making a subjective judgement. This is labour intensive, and concentration problems can lead to errors. Additionally, gradual changes and changing shades due to variable light conditions are confusing and difficult for humans to detect.

Several wood recognition systems using grey-scale textural features and laboratory measurement setups were proposed. A wood recognition system using macroscopic camera setup, neural networks classifier and grey-level co-occurrence matrix features is specified in [6]. This system requires large number ($\approx$ 100) of training images per wood class. Papers [2,12] report similar systems using also grey-level or rotational invariant grey-level co-occurrence matrix

G. Azzopardi and N. Petkov (Eds.): CAIP 2015, Part I, LNCS 9256, pp. 300–311, 2015.
DOI: 10.1007/978-3-319-23192-1_25

features and correlation based classifier. A comparative study [11] reports better performance of the Gabor features over the co-occurrence matrix features. Finally, [15] combines the Gabor and the co-occurrence matrix features for the neural networks classifier. All these systems ignore textural spectral information, use obsolete textural features, and require good quality visual measurements with fixed illumination conditions.

As an alternative, we have developed an application to identify wood species using a smartphone camera, which returns the resulting species name and a corresponding high quality database wood specimen image. This computer-aided wood identification system retrieves a wood template from a digital wood database, selecting that which most closely resembles the query sample. A wooden surface is captured by a smartphone camera with the developed Android application, and the image is transmitted to the server side which computes the advanced multispectral Markovian textural features and finds the most similar wood species from its database. The Markovian features are not only very efficient, compacting the representation of visual wood properties, but they are simultaneously invariant to illumination colour, robust to illumination heterogeneity, and illumination direction, therefore the retrieval result is not influenced by the unknown and variable illumination properties. Thus we assume that the wooden texture can be approximated by a surface reflectance field model [4], i.e., bidirectional texture function with fixed or small viewing angle changes. The recognized wood species together with its high quality database pattern is sent back to the user so he or she can verify the classifiers result. The challenging part of the method is to compare poor quality smartphone images taken under variable illumination and resolution conditions with high quality high resolution matte wooden textures stored in the wood database.

2 Markovian Textural Features

Our texture analysis is based on spatial and multimodal relations modelling by a wide-sense Markovian model. We employ a Causal Autoregressive Random (CAR) model, because it allows very efficient analytical estimation of its parameters. Subsequently, the estimated model parameters are transformed into illumination/colour invariants, which characterize the corresponding wooden texture. These colour invariants encompass inter-spectral (in the case of full 3D CAR model) and spatial relations in the texture which are bounded to a selected contextual neighbourhood (see Fig. 1). Wood veneers with similar structure and spectral properties produce similar features.

Texture Model

Let us assume that multispectral texture image is composed of C spectral planes (usually $C = 3$ for colour images). $Y_r = [Y_{r,1}, \ldots, Y_{r,C}]^T$ is the multispectral pixel at location r, where the multiindex $r = [r_1, r_2]$ is composed of r_1 row and r_2 column index, respectively. The spectral planes are modelled using a set of C 2-dimensional CAR models. The set of 2D models is used instead of full 3D

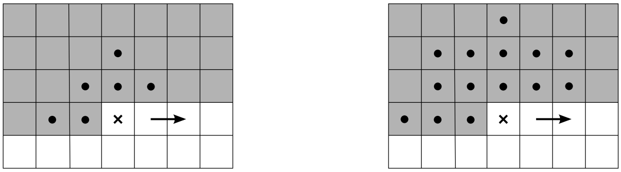

Fig. 1. Examples of contextual neighbourhood I_r. From the left, it is the unilateral semi-hierarchical neighbourhood of third and sixth order. X marks the current pixel, the bullets are pixels in the neighbourhood, the arrow shows movement direction, and the grey area indicates acceptable neighbourhood pixels.

model, because images from smarthone cameras had degradated interspectral relations.

The CAR representation assumes that the multispectral texture pixel Y_r can be modelled as a linear combination of its neighbours:

$$Y_r = \gamma Z_r + \epsilon_r \ , \qquad Z_r = [Y_{r-s}^T : \forall s \in I_r]^T \tag{1}$$

where Z_r is the $C\eta \times 1$ data vector with multiindices r, s, $\gamma = [A_1, \ldots, A_\eta]$ is the $C \times C\,\eta$ unknown parameter matrix with square sub-matrices A_s. Some selected contextual causal or unilateral neighbour index shift set is denoted I_r and $\eta = \mathit{cardinality}(I_r)$, see Fig. 1. A unilateral neighbourhood I_r (the left upper orientation) is defined as $I_r \subset I_r^U = \{s : s_1 < r_1 \ \mathit{or}\ (s_1 = r_1, s_2 < r_2)\}$ and similarly ([3]) its subset - the causal neighborhood. The neighborhood order is based on the Euclidean distance from r. The white noise vector ϵ_r has normal density with zero mean and unknown diagonal covariance matrix, same for each pixel. In the case 2D CAR models stacked into the model equation (1) the uncorrelated noise vector components ϵ_r are assumed and the parameter matrices A_s are diagonal.

The texture is analysed in a chosen direction, where multiindex t changes according to the movement on the image lattice. Given the known history of CAR process $Y^{(t-1)} = \{Y_{t-1},\ Y_{t-2}, \ldots, Y_1, Z_t,\ Z_{t-1}, \ldots, Z_1\}$ the parameter estimation $\hat{\gamma}$ for the given pixel position can be computed using statistics [3]:

$$\begin{aligned}
\hat{\gamma}_{t-1}^T &= V_{zz(t-1)}^{-1}\, V_{zy(t-1)} \ , \\
V_{t-1} &= \begin{pmatrix} \sum_{u=1}^{t-1} Y_u {Y_u}^T & \sum_{u=1}^{t-1} Y_u {Z_u}^T \\ \sum_{u=1}^{t-1} Z_u {Y_u}^T & \sum_{u=1}^{t-1} Z_u {Z_u}^T \end{pmatrix} + V_0 = \begin{pmatrix} V_{yy(t-1)} & V_{zy(t-1)}^T \\ V_{zy(t-1)} & V_{zz(t-1)} \end{pmatrix} \ , \\
\lambda_{t-1} &= V_{yy(t-1)} - V_{zy(t-1)}^T V_{zz(t-1)}^{-1} V_{zy(t-1)} \ ,
\end{aligned} \tag{2}$$

where the positive definite matrix V_0 represents a prior knowledge, see [3] for details. Moreover, the parameter estimate can be efficiently computed for all pixel positions using a numerically robust recursive formula [3], which is advantageous for texture segmentation applications. Finally, the optimal contextual neighbourhood I_r can be found analytically by maximising the corresponding posterior probability [3].

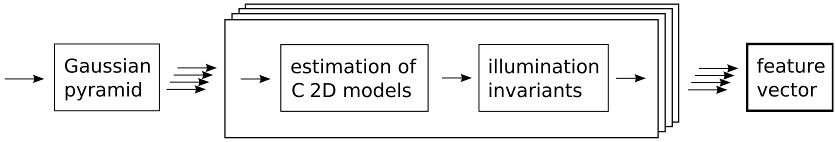

Fig. 2. The texture analysis algorithm flowchart using a set of 2D random field models.

Colour Invariant Features

Colour invariants are computed from the CAR parameter estimates to make them independent on changes of illumination intensity and colours. Moreover, our invariants are approximately invariant to infrequent changes of local illumination intensity and experiments show their robustness to variation of illumination direction (see [13,14] for details). For 2D models, their definition is the following:

1. trace: $\operatorname{tr} A_s, \ \forall s \in I_r$,
2. diagonals: $\nu_s = \operatorname{diag} A_s , \quad \forall s \in I_r$.
3. α_1: $1 + Z_r^T V_{zz}^{-1} Z_r$,
4. α_2: $\sqrt{\sum_r \left(Y_r - \hat{\gamma} Z_r\right)^T \lambda^{-1} \left(Y_r - \hat{\gamma} Z_r\right)}$,
5. α_3: $\sqrt{\sum_r \left(Y_r - \mu\right)^T \lambda^{-1} \left(Y_r - \mu\right)}$, μ is the mean value of vector Y_r ,

where the invariants $\alpha_1 - \alpha_3$ are computed for each spectral plane separately. The model parameters $\hat{\gamma}$, λ are estimated using formula (2), we omit subscstripts for simplicity. Feature vectors are formed from these illumination invariants, which are easily evaluated during the CAR parameters estimation process.

Algorithm

The texture analysis algorithm starts with factorisation of texture image into K levels of the Gaussian down-sampled pyramid and subsequently each pyramid level is modelled by the CAR model. The pyramidal factorization is used, because it enables model to easily capture larger spatial relations. We usually use $K = 4$ levels of the Gaussian pyramid, if the image size is sufficient (at least 400×400) it is possible to improve performance with the additional pyramid level $(K = 5)$.

Although the optimal neighbourhood of the CAR model can be optimally selected, practically, we use the 6-th order semi-hierarchical neighbourhood (cardinality $\eta = 14$), see Fig. 1 for details. This neighbourhood size provides good combination of sufficient support and stable model parameters, which do not varies for similar textures. Finally, the estimated parameters for all pyramid levels are transformed into the colour invariants and concatenated into a common feature vector. The algorithm scheme is depicted in Fig. 2.

The dissimilarity between two feature vectors of two textures T, S is computed using fuzzy contrast [10] in its symmetrical form FC_3.

3 Alternative Textural Features

Numerous textural features were published which can be used with greater or lesser success for wooden texture classification. The proposed Markovian textural features applied to veneer recognition were compared with efficient and widely used alternative Local Binary Patterns (LBP) [8] and Gabor textural features [1,7,9]. Results of the Opponent Gabor features [5] were inferior, so that they are not included in the paper.

3.1 Local Binary Patterns

Local Binary Patterns [8] are histograms of texture micro patterns. For each pixel, a circular neighbourhood around the pixel is sampled, P is the number of samples and R is the radius of circle. The sampled point values are thresholded by the central pixel value and the pattern number is formed:

$$LBP_{P,R} = \sum_{s=0}^{P-1} \operatorname{sgn}(Y_s - Y_c)\, 2^s , \qquad (3)$$

where *sgn* is the sign function, Y_s is the grey value of the sampled pixel, and Y_c is the grey value of the central pixel. Subsequently, the histogram of patterns is computed. Because of the thresholding, the features are invariant to any monotonic grey-scale change. The multiresolution analysis is done by growing of the circular neighbourhood size. All LBP histograms were normalised to have unit L_1 norm. The similarity between LBP feature vectors is measured by means of Kullback-Leibler divergence as the authors suggested.

We have tested features $\text{LBP}_{8,1+8,3}$, which are combination of features with radii 1 and 3. They were computed either on gray images or on each spectral plane of color image and concatenated. We also tested uniform version $\text{LBP}^u_{16,2}$, but their results were inferior.

3.2 Gabor Features

The Gabor filters [1,7,9] can be considered as orientation and scale tunable edge and line (bar) detectors and statistics of Gabor filter responses in a given region are used to characterize the underlying texture information. A two dimensional Gabor function $g(r_1, r_2) : \Re^2 \rightarrow \mathcal{C}$ can be specified as

$$g(r_1, r_2) = \frac{1}{2\pi\sigma_{r_1}\sigma_{r_2}} \exp\left[-\frac{1}{2}\left(\frac{r_1^2}{\sigma_{r_1}^2} + \frac{r_2^2}{\sigma_{r_2}^2}\right) + 2\pi i W r_1\right] , \qquad (4)$$

where $\sigma_u = \frac{1}{2\pi\sigma_{r_1}}$, $\sigma_v = \frac{1}{2\pi\sigma_{r_2}}$, and $\sigma_{r_1}, \sigma_{r_2}$ are filter parameters. $\sigma_{r_1}, \sigma_{r_2}$ are variances in r_1, r_2 directions and W is a modulation frequency parameter. Gabor wavelet transform is defined as

$$W_{mn}(r_1, r_2) = \int Y(s_1, s_2)\, g^*_{mn}(r_1 - s_1, r_2 - s_2)\, ds_1 ds_2 , \qquad (5)$$

where $*$ indicates the complex conjugate. The Gabor features are defined as the mean μ_{mn} and the standard deviation σ_{mn} of the magnitude of transform coefficients.

4 Experiments

The performance of our application was verified on the wood database, which contains veneers from varied European and exotic wood species, each with two sample images only. The training set included images of 66 wood species acquired by a colour scanner device, while the test set was composed of images of 59 wood species acquired by two different smartphones (HTC Desire S and Samsung Galaxy S3). The training set was acquired with controlled condition (stable illuminations source, aligned position) provided by the scanning machine. On the contrary, the test set was captured from a hand without controlled conditions, however, the images were taken from approximately the same distance and with orientation approximately with the material sample to limit unnecessary variations. All images were resized to 767×1024 pixels aspect ratio were maintained and redundant pixels were discarded. Lanczos interpolation was employed in image resize.

We have performed three wood veneers recognition experiments. Naturally, the proposed textural features and the alternatives were compared in the exactly same conditions. The computed feature vectors were compared with author suggested distances and classified using the Nearest Neighbour (1-NN) classifier.

4.1 Experiment 1

In the first experiment, we tested recognition of whole images captured by two mobile phones against training database acquired by the scanner. Separately, we tested images acquired by the mobile phones with the internal flash ON and OFF, see examples in Fig. 3. Each of these four setups included 59 test images.

Tab. 1 displays the results, where the recognition accuracy of the images without flash were worse for all features. The reason is that (a) the images captured without flash were more blurry (caused by small smartphones lenses and sensors) (b) additionally, CAR features cancel uneven illumination present in images with flash. Worse results of the HTC smartphone were caused probably by its very aggressive JPEG compression, which cannot be adjusted in the used device model.

Figs. 4–7 illustrate the systems typical performance applied to European (Figs. 4, 5) and exotic wood (Figs. 6, 7) samples. Fig. 4 illustrates retrieval results of our method - the most probable results were both apple samples, which is correct, and the third result was the closest pear wood specimen. In the same figure, the LBP features retrieved wrongly all three most probable results (twice a bamboo sample and the macassar wood).

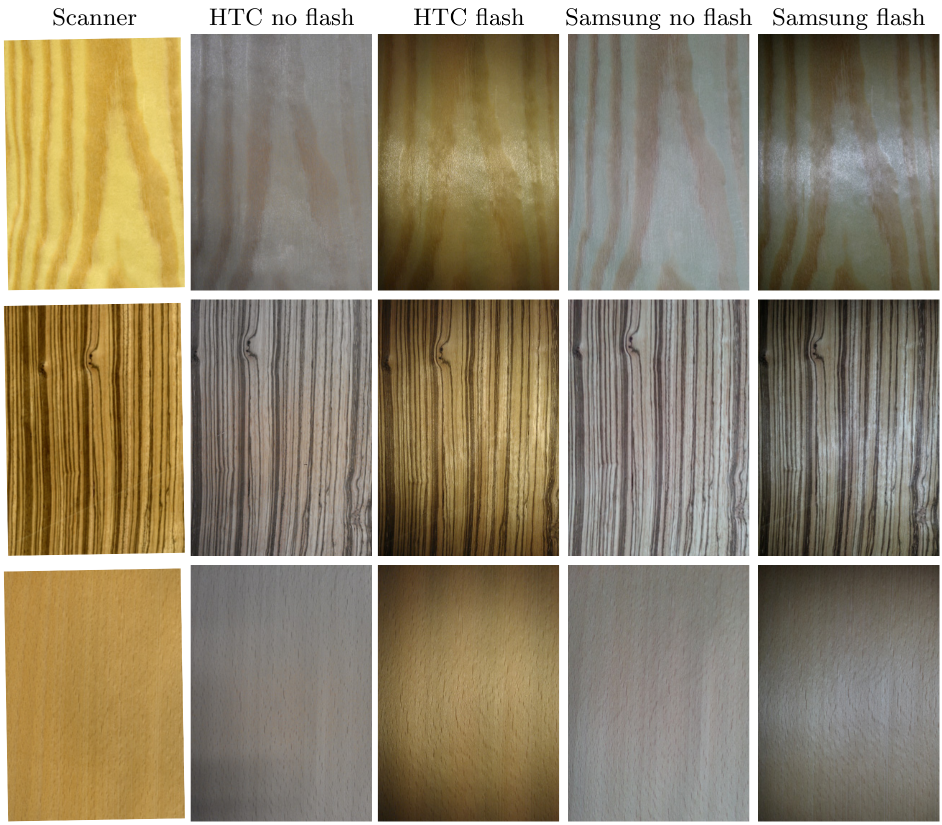

Fig. 3. Images of the following veneer samples: pine, zebrano, and beech, respectively. The columns correspond to different acquisition setups.

Table 1. Experiment 1, recognition accuracy [%] of whole veneers by both smartphones.

	HTC flash	HTC	Samsung flash	Samsung
Gabor colour	28.6	8.1	36.7	26.5
LBP gray	24.5	8.2	34.7	16.3
LBP colour	20.4	8.2	38.8	18.4
2D CAR	59.2	30.6	79.6	63.4
2D CAR ($K = 5$)	**65.3**	40.8	**81.6**	67.7

4.2 Experiment 2

In the second experiment, we tested ability of textural features to generalize and to recognize different parts of material sample. The setup was almost the same as in the Experiment 1 with the exception that both test and training set was

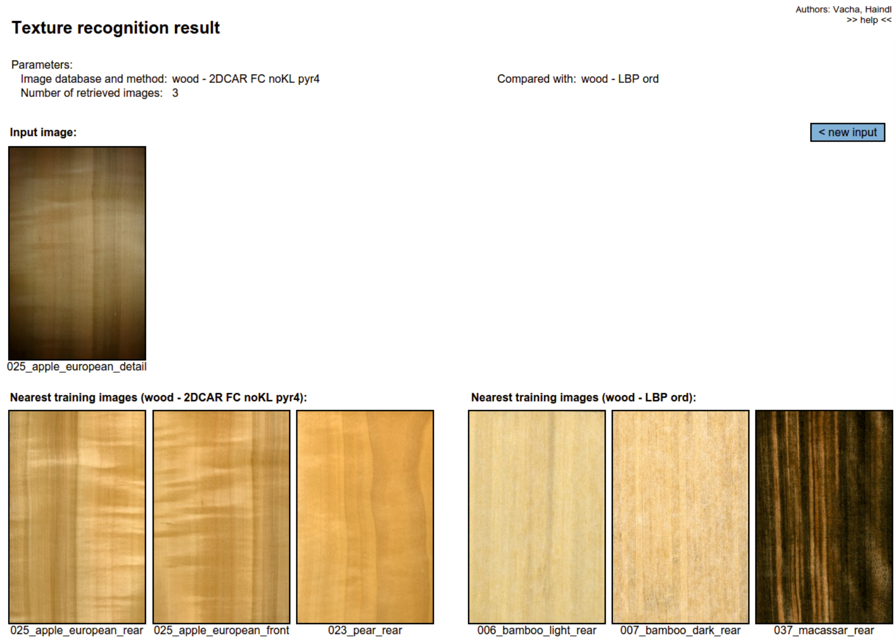

Fig. 4. An apple wood sample taken by a smartphone camera and the three closest query results using either Markovian or LBP textural features.

composed of upper half and lower half of the original images. The recognition was performed "across" halfs, i.e., in two sub-experiments: (a) trained on upper halfs from the scanner, tested on the lower halfs from a mobile; (b) trained on the lower halfs from the scanner, tested on the upper halfs from a mobile. The results of these two sub-experiments, each with 59 test images, were averaged.

The results are summarized in Tab. 2, where the recognition accuracy of images without flash were excluded as they were inferior for all tested features (consistently with the Experiment 1).

4.3 Experiment 3

In the third experiment, we tested classification of upper against lower parts similarly as in the Experiment 2, however, both training and test images were from the same acquisition device. Again, the recognition accuracy was evaluated for 2×59 test images. The purpose of this experiment was to asses, what is the cause of the performance degradation.

The results are displayed in Tab. 3. Recognition accuracy 100%, in the upper left corner, means that 2D CAR features extract important textural properties as they are able to perfectly recognise different parts of the same veneer sample. In fact, this is true for all tested features as the recognition accuracy was always between 99% and 100%. When compared with the results in Experiment 2,

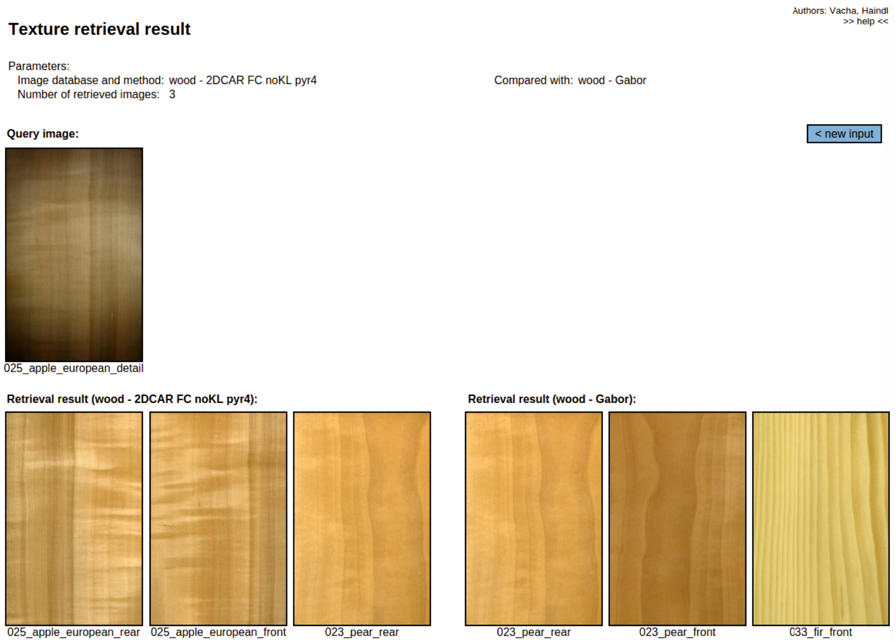

Fig. 5. The apple wood sample taken by a smartphone camera and the three closest query results using either Markovian or Gabor textural features.

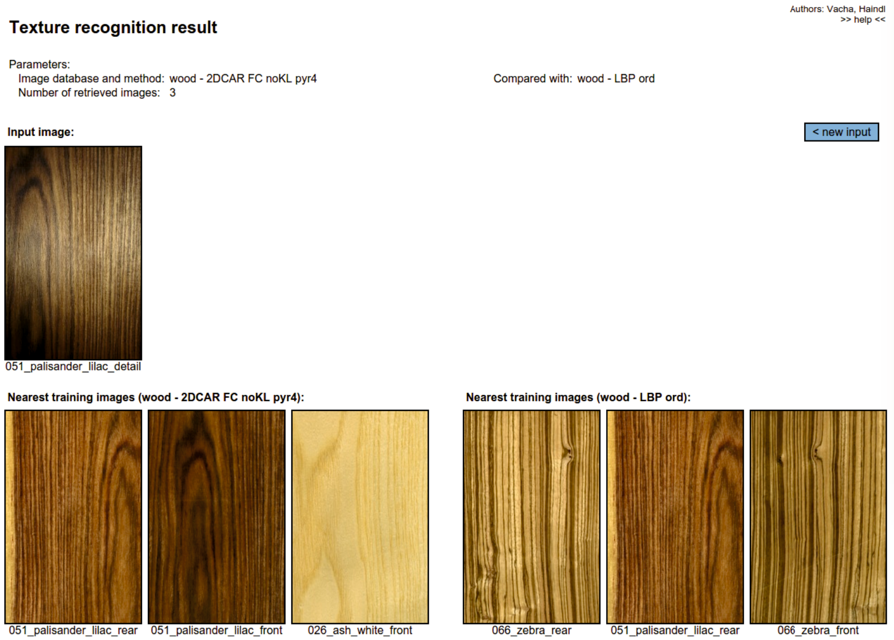

Fig. 6. A palisander wood retrieval results comparison between the Markovian and LBP features.

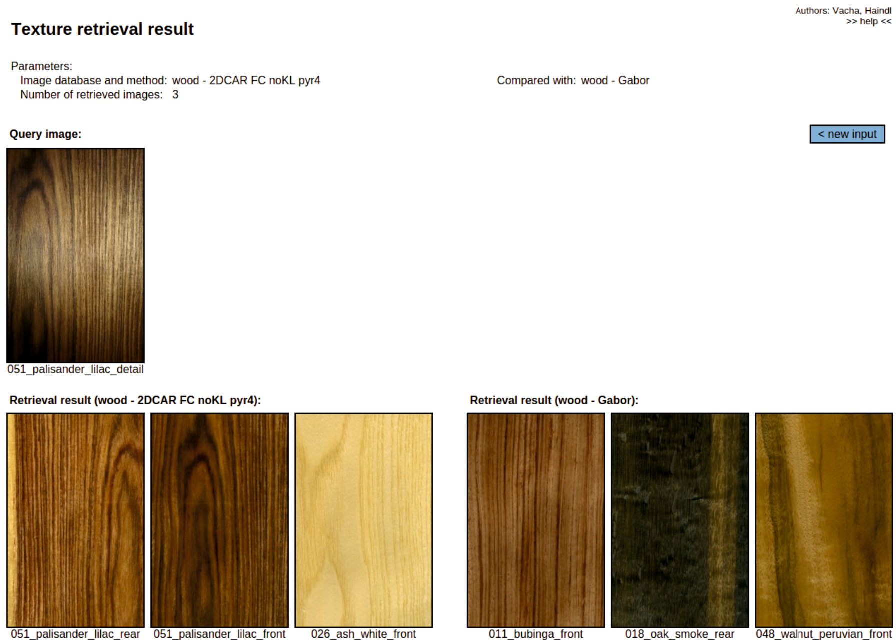

Fig. 7. The palisander wood retrieval results comparison between the Markovian and Gabor features.

Table 2. Experiment 2, recognition accuracy [%] of different veneer parts by the smartphones.

	HTC flash	Samsung flash
LBP gray	29.6	40.8
LBP colour	29.6	48.0
2D CAR	46.9	69.4
2D CAR ($K = 5$)	**49.0**	**66.3**
Gabor color	18.3	27.5

it implies that about 30% of recognition accuracy for 2D CAR features were lost, probably, by combination of two factors: (a) poor quality of smartphone cameras, (b) scale and other variations introduced by acquisition from hand. (For the simplicity, the rest of the first column is left empty, since the results are included in the Experiment 2.)

To examine more carefully the previous claim about performance lost, the rest of the table displays results with changing training and testing combinations of the smartphones (still different half of the veneer sample was used for test and training). Very good results on the diagonal (89.9% and 94.9%) implies that degradation by smartphone cameras are consistent. We can speculate that remaining 7–10% of performance was lost due to image acquisition from hand.

Table 3. Experiment 3, recognition accuracy [%] of different veneer parts, but with the same acquisition device (in bold). The results are for 2D CAR, the test set devices are in rows, while training set devices are in columns.

	Scanner	HTC flash	Samsung flash
Scanner	**100**		
HTC flash		**89.8**	78.6
Samsung flash		83.7	**94.9**

More interestingly, Tab. 3 is not symmetric, it seems that better sensor/camera combination is more important for the test set.

5 Conclusion

Our colour invariant Markovian textural features were successfully applied for recognition of wood veneers using a smartphone. The method's correct recognition accuracy improvements are about 40% and 20% (Experiment 2), compared to the Local Binary Patterns (LBP) features, which is the best alternative from all tested standard textural features. However, the actual performance is highly dependent on the acquisition device, as demonstrated by 15% performed drop for camera in HTC Desire S compared to Samsung Galaxy S3. In general, smartphone cameras have sufficient resolution (up to 10 mega pixels), however, their poor quality lenses and aggressive JPEG compression result in inferior image quality and thus a more demanding recognition task. Nevertheless, our high correct recognition rate (82%), suggests that the proposed method can be successfully used in various practical wood recognition applications.

The results can be reviewed in an online demonstration[1], which shows retrieval using images from mobile phones as queries.

Acknowledgments. This research was supported by the Czech Science Foundation project GAČR 14-10911S.

References

1. Bovik, A.: Analysis of multichannel narrow-band filters for image texture segmentation. IEEE Trans. on Signal Processing **39**(9), 2025–2043 (1991)
2. Bremananth, R., Nithya, B., Saipriya, R.: Wood species recognition using glcm and correlation. In: International Conference on Advances in Recent Technologies in Communication and Computing. ARTCom 2009, pp. 615–619. IEEE (2009)
3. Haindl, M.: Visual data recognition and modeling based on local markovian models. In: Florack, L., Duits, R., Jongbloed, G., Lieshout, M.C., Davies, L. (eds.) Mathematical Methods for Signal and Image Analysis and Representation, Computational Imaging and Vision, chap. 14, vol. 41, pp. 241–259. Springer, London (2012). doi:10.1007/978-1-4471-2353-8_14. http://dx.doi.org/10.1007/978-1-4471-2353-8_14

[1] http://cbir.utia.cas.cz/veneers/

4. Haindl, M., Filip, J.: Visual Texture. Advances in Computer Vision and Pattern Recognition. Springer-Verlag London, London (January 2013)
5. Jain, A., Healey, G.: A multiscale representation including opponent colour features for texture recognition. IEEE Transactions on Image Processing **7**(1), 124–128 (1998)
6. Khalid, M., Lee, E.L.Y., Yusof, R., Nadaraj, M.: Design of an intelligent wood species recognition system. International Journal of Simulation System, Science and Technology **9**(3), 9–19 (2008)
7. Manjunath, B.S., Ma, W.Y.: Texture features for browsing and retrieval of image data. IEEE Transactions on Pattern Analysis and Machine Intelligence **18**(8), 837–842 (1996)
8. Ojala, T., Pietikäinen, M., Mäenpää, T.: Multiresolution gray-scale and rotation invariant texture classification with local binary patterns. IEEE Transactions on Pattern Analysis and Machine Intelligence **24**(7), 971–987 (2002)
9. Randen, T., Husøy, J.H.: Filtering for texture classification: A comparative study. IEEE Transactions on Pattern Analysis and Machine Intelligence **21**(4), 291–310 (1999)
10. Santini, S., Jain, R.: Similarity measures. IEEE Transactions on Pattern Analysis and Machine Intelligence **21**(9), 871–883 (1999)
11. Tou, J.Y., Tay, Y.H., Lau, P.Y.: A comparative study for texture classification techniques on wood species recognition problem. In: Fifth International Conference on Natural Computation. ICNC 2009, vol. 5, pp. 8–12. IEEE (2009)
12. Tou, J.Y., Tay, Y.H., Lau, P.Y.: Rotational invariant wood species recognition through wood species verification. In: First Asian Conference on Intelligent Information and Database Systems. ACIIDS 2009, pp. 115–120. IEEE (2009)
13. Vacha, P., Haindl, M.: Image retrieval measures based on illumination invariant textural MRF features. In: Sebe, N., Worring, M. (eds.) Proceedings of ACM International Conference on Image and Video Retrieval, CIVR 2007, pp. 448–454. ACM, July 9–11, 2007
14. Vácha, P., Haindl, M.: Texture recognition using robust Markovian features. In: Salerno, E., Çetin, A.E., Salvetti, O. (eds.) MUSCLE 2011. LNCS, vol. 7252, pp. 126–137. Springer, Heidelberg (2012)
15. Yusof, R., Rosli, N.R., Khalid, M.: Using gabor filters as image multiplier for tropical wood species recognition system. In: 2010 12th International Conference on Computer Modelling and Simulation (UKSim), pp. 289–294. IEEE (2010)